Trioctahedral Clay Mineral Assemblages in Paleozoic Marine Evaporite Rocks

Marc W. Bodine, Jr.
U.S. Geological Survey
Denver, Colorado, USA

ABSTRACT

Clay-mineral assemblages from the Upper Silurian Retsof salt bed of the Salina Group in western New York State, the Middle Pennsylvanian Paradox Member of the Hermosa Formation in eastern Utah, and the Upper Permian Castile and Salado Formations in southeastern New Mexico consist chiefly of Mg-rich trioctahedral clays. Except for variable quantities of illite the dioctahedral clays are absent. Trioctahedral clay species include: chlorite; interstratified chlorite-trioctahedral smectite with regular interstratification (corrensite) to random interstratification; trioctahedral smectite; interstratified talc-trioctahedral smectite; talc; and serpentine.

The distinctive mineralogy of the clay assemblages strongly suggests an authigenic origin. Recrystallization and Mg-metasomatism of "average" clay detritus to Al-bearing trioctahedral clays is to be expected in response to increased Mg^{2+} activity in marine evaporite brines. Somewhat more speculative conclusions are: (1) talc and serpentine crystallized from evaporite brines with speciation a function of the $Mg^{2+}/(H^{+})^2$ ion activity ratio; and (2) interstratified talc-trioctahedral smectite, associated only with polyhalite beds, resulted from Al-leaching of interstratified chlorite-trioctahedral smectite during diagenetic replacement of calcium sulfate by polyhalite.

INTRODUCTION

In their classic systematic study of clay minerals in the German Zechstein Formation, Füchtbauer and Goldschmidt (1959) suggested that the marine hypersaline depositional environment played a major role in the genesis of the clay mineral assemblages. Subsequent studies of Zechstein clays by Niemann (1960), Dreizler (1962), Pundeer (1969), and others, and clay mineral investigations at other marine evaporite localities by Echle (1961), Droste (1963), Lounsbury (1963), Lippmann and Savascin (1969), Bodine and Standaert (1977), and Bodine (1978), among others, as well as discussions in important review monographs (Borchert and Muir, 1964; Kühn, 1968; Millot, 1970; Braitsch, 1971) have, for the most part, amplified and strengthened this conclusion.

The mineralogy and geochemistry of clay mineral assemblages from three North American marine evaporite deposits are discussed in this paper toward further documenting the importance of the depositional environment in the formation of these distinctive and unusual clay mineral assemblages. Furthermore, features of specific clay minerals and their associations with the evaporite strata prompt two intriguing speculations on clay-forming processes in depositional and diagenetic environments of hypersaline rocks.

The three Paleozoic marine evaporite deposits are (Figure 1): the Upper Permian (Ochoan) Salado and uppermost Castile Formations from the ERDA-9 drill core at the Waste Isolation Pilot Plant (WIPP) site in southeastern New Mexico; the Middle Pennsylvanian Paradox Member of the Hermosa Formation from the Gibson Dome No. 1 drill core in the Paradox basin of southeastern Utah; and an Upper Silurian (Cayugan) Salina Group halite bed in the Retsof Mine in western New York State.

GEOLOGIC SETTING

Each of the three localities provides well-documented marine evaporite sections with characteristic saline mineral successions; however, they do differ one from another. They differ in geologic age, paleogeography of the detrital source and depositional environments, extent of progressive evaporation, and character and extent of postdepositional pore-fluid mobility and salt metasomatism (Table 1).

ERDA-9 drill core. ERDA-9 was drilled as part of geologic characterization studies of the proposed WIPP repository site in Ochoan salts (Powers and others, 1978).

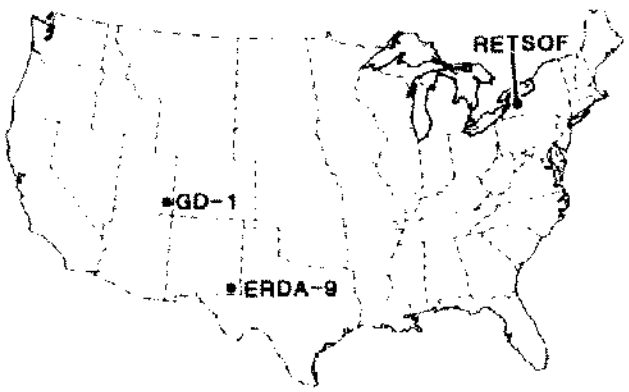

Figure 1. Index map of the United States locating ERDA-9 drill hole in the Delaware Basin, Gibson Dome No. 1 (GD-1) drill hole in the Paradox Basin, and the Retsof Mine in the Appalachian Basin.

The hole is located in the Delaware Basin on the repository tract (sec. 20, T. 22 S., R. 31 E.) in eastern Eddy County about 47 km east of Carlsbad, New Mexico (Figure 2).

Ochoan rocks at the WIPP site (Figure 3) are 1227 m thick of which the upper 857 m were cored in ERDA-9. The Castile Formation is the basal Ochoan unit and overlies the deepwater marine clastics and carbonates of the Guadalupian Bell Canyon Formation. The Castile Formation is 383 m thick and consists of thick anhydrite intervals intercalated with nearly equally thick rock-salt intervals. The continuity of sharply defined, thin lamina or varves in the anhydrites (Anderson and others, 1972) suggest deepwater deposition for most of the Castile Formation. Only the uppermost 12.5 m of the upper anhydrite interval of the Castile Formation was cored in ERDA-9.

The overlying Salado Formation is 602 m thick in ERDA-9 and consists chiefly of bedded halite (85–90 percent) with thin interbeds of anhydrite, polyhalite, fine clastics, and potash-bearing soluble salt assemblages (Figure 3). Three members are recognized (Jones, 1973); unnamed upper and lower members; and an intervening middle member, the McNutt potash zone. The members

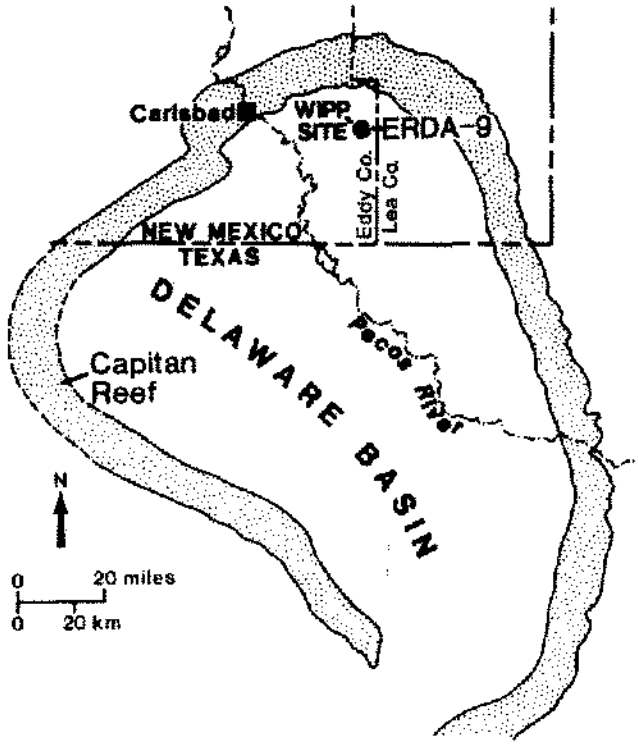

Figure 2. Location map of the Delaware Basin showing the Capitan Reef, the WIPP site, and the ERDA-9 drill hole from Anderson (1982).

are nearly identical except the McNutt potash zone contains beds with soluble potash salts, chiefly sylvite, langbeinite, and carnallite, which are absent from the upper and lower members. Throughout the Salado Formation, there is an irregularly developed and frequently repeated cyclicity; an ideal cycle contains a basal parting of claystone overlain by anhydrite or polyhalite and a thick halite interval with or without potassium minneral-bearing beds. Textural and mineralogic features (Powers and others, 1978) strongly suggest relatively shallow depositional conditions throughout most of Salado sedimentation.

TABLE 1

Summary of Geologic Features of ERDA-9, Gibson Dome No. 1, and Retsof Mine Evaporites

	ERDA-9		Gibson Dome 1	Retsof Mine
Location	SE. New Mexico		SE. Utah	W. New York
Sedimentary basin	Delaware		Paradox	Appalachian
Geologic age	Upper Permian		M. Pennsylvania	U. Silurian
Formation	Castile Formation	Salado Formation	Hermosa Formation Paradox Member	Vernon Formation
Maximum evaporation	Halite	K salts	K salts	Halite
Detrital source	Moderate	Near/moderate	Near/moderate	Distant
Detrital influx	Low	Moderate	Moderate	Abundant
Brine depth	Deep/moderate	Shallow	Moderate	Shallow
Salt diagenesis	(?) Minor	Substantial	Minor	Minor

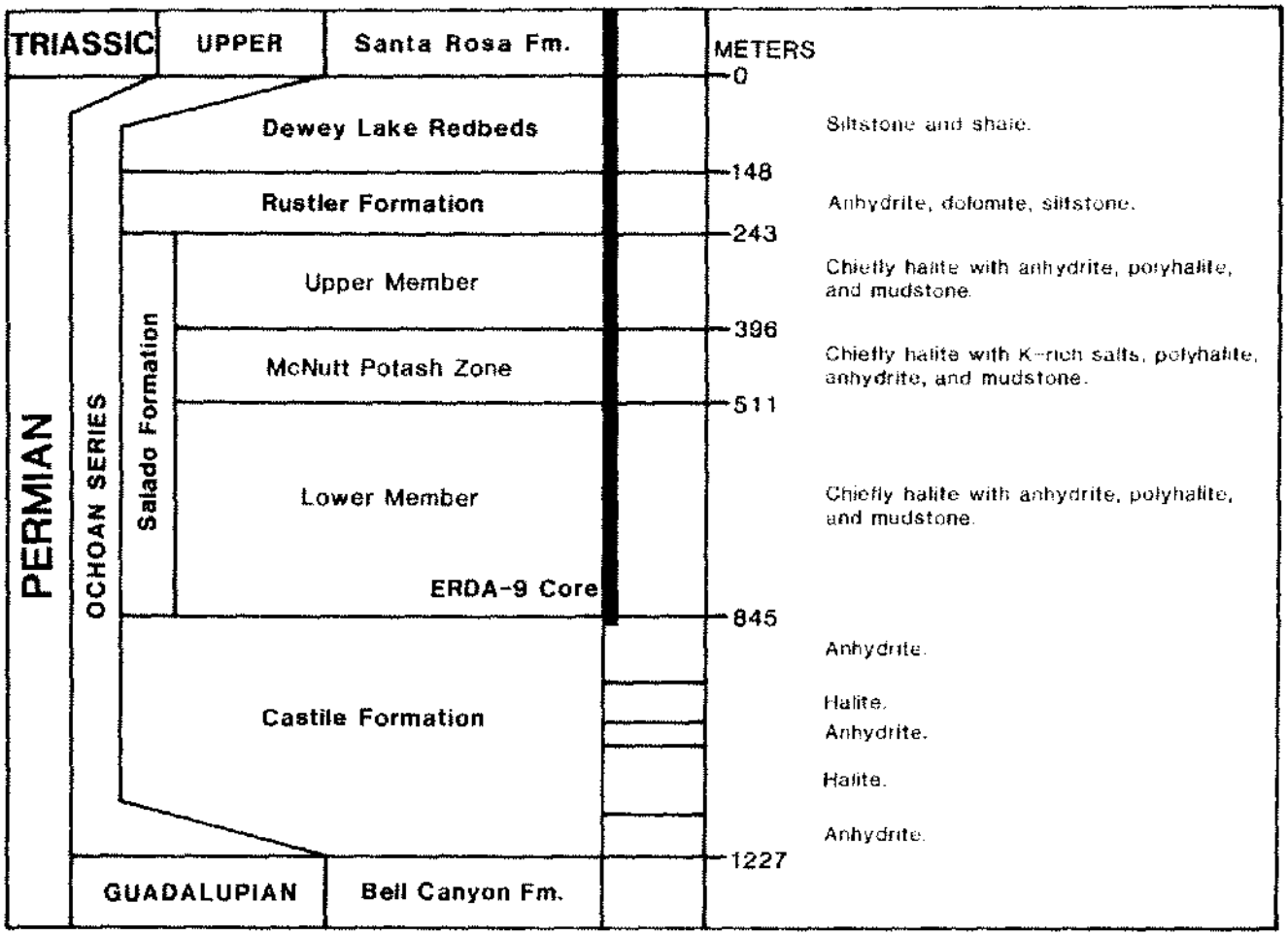

Figure 3. Generalized stratigraphic column of Ochoan rocks at the WIPP site, Eddy County, New Mexico and the cored interval in the ERDA-9 drill hole (Powers and others, 1978).

The Rustler Formation and Dewey Lake Red beds overlie the Salado Formation (Figure 3) and reflect progressively decreasing salinity and increasing detrital influx into the basin. With cessation of Ochoan sedimentation, no further deposition occurred until the Late Triassic when the Santa Rosa Formation was deposited.

Changing Ochoan paleogeography strongly influenced the character of these evaporites (Anderson and others, 1972; Powers and others, 1978). Castile deposition was restricted to the Delaware Basin within the seaward confines of the imposing relict Guadalupian Capitan reef (Figure 3). As the deep basin filled with evaporite sediments, conditions shoaled toward the end of Castile sedimentation; furthermore, transgression over the reef's northern and eastern rim resulted in deposition of Salado salts extending onto back reef flats of the relict reef system. It appears that during Castile sedimentation the reef barred appreciable detrital influx into the basin interior, but during Salado deposition with evaporite sedimentation overlapping segments of the reef, the influx of detritus into the basin increased markedly and continued to increase during Rustler and Dewey Lake sedimentation.

There is also general agreement (Powers et al. 1978) that the many polyhalite beds in the Salado Formation are secondary replacements of primary calcium sulfate; a process which apparently occurred early in the postdepositional history of the salts. Frequent anomalies of substantial bromine depletion in many Salado halites (Adams, 1969), the apparent extensive Mg-depletion in the McNutt potash zone, and the occurrence of magnesite as the dominant Salado carbonate (Jones, 1973) are further indicators of extensive diagenetic dissolution, salt recrystallization, and metasomatism.

Gibson Dome No. 1 drill core. Gibson Dome No. 1 in the Paradox Basin was also drilled as part of geologic characterization study of a proposed underground nuclear waste repository site (Woodward-Clyde Consultants, 1982). The hole is located 24 km east of the confluence of

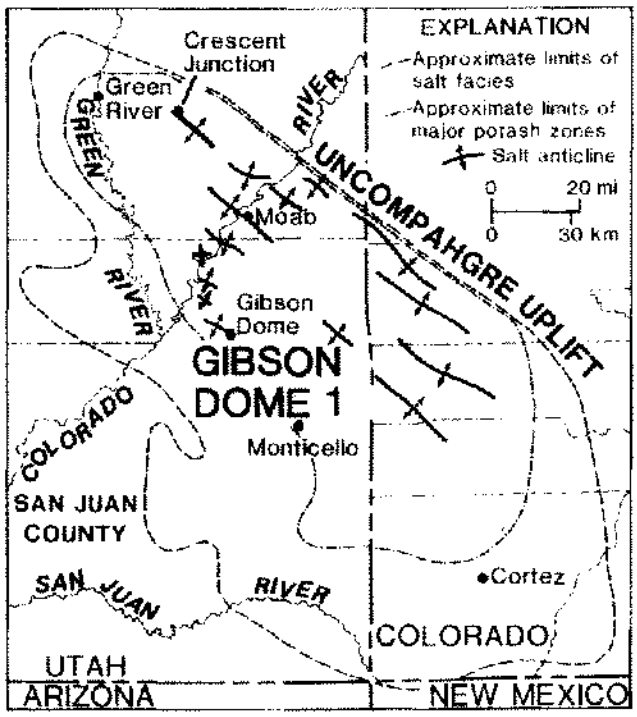

Figure 4. Location map of the Gibson Dome No. 1 drill hole in the Paradox Basin showing limits of salt and potash beds in the Paradox Member of the Hermosa Formation from Hite and Buckner (1981).

the Colorado and Green Rivers (Figure 4) in San Juan County, Utah (sec. 21, T. 30 S., R. 21 E.).

The hole (Woodward-Clyde Consultants, 1982) was drilled to a depth of 1945.9 m of which the lower 1819 m were cored. The core bottoms in the Mississippian-Devonian Ouray Limestone and extends upward through the Mississippian Leadville Limestone, the Pennsylvanian Molas and Hermosa Formations, and the lower 378 m of undifferentiated Cutler Group rocks (Figure 5).

The Paradox Member of the Hermosa Formation is nearly 800 m thick in Gibson Dome No. 1 and consists chiefly of rock salt with thinner interbeds of clastics and other marine evaporite lithologies (Figure 5). The underlying lower member consists of normal marine limestones in the lower part which grade upward into a succession of interbedded anhydrites, dolomites, and limestones reflecting a transition to hypersaline sedimentation. The overlying upper member consists of anhydritic strata which grade upward into a normal marine sequence of interbedded shallow-water carbonates and clastics.

Hite (1960) described a cyclicity within the Paradox salts which permits basin-wide correlation of 29 individual cycles. Twenty of these cycles are specifically identified in the Gibson Dome No. 1 core (Figure 5). A typical cycle consists of relatively thin intercalated beds of anhydrite, dolomite, and black shale overlain by a thick interval of bedded halite with or without interbeds of K-rich salt assemblages. Each cycle was deposited on a pronounced dissolution surface developed on the salt of the previous cycle.

Hite and Buckner (1981) have suggested the cyclicity parallels eustatic rise and fall of sea level in response to alternating periods of Pennsylvanian glacial retreat and advance. With rising sea level, the barrier to the basin was flooded and the basin was recharged with seawater; with falling sea level, the barrier was reestablished and evaporation produced the characteristic succession of marine salts. The preservation of fine bedding with anhydrite lamellae in the halite, the lack of oxidation in the black shales, and the preservation of organic matter throughout the section indicate deposition in moderately deep water below wave base and preclude periods of desiccation. Salt dissolution at the end of each cycle apparently was subaqueous and occurred when salt-undersaturated normal seawater entered the basin and diluted the pre-existing salt-saturated brine. In those few cycles (Figure 5) where a zone rich in potassium minerals, chiefly sylvite, is observed, O. B. Raup (written commun.) suggests the primary assemblage—most likely halite-carnallite-kieserite—was selectively leached of magnesium by these same more dilute brines leaving a sylvite-halite residue.

Except for this very early diagenetic dissolution and selective leaching of magnesium associated with cyclic seawater recharge, it appears that no more than negligible postdepositional salt dissolution, recrystallization, and metasomatism occurred. This is based on the preservation of nearly ideal primary bromine profiles throughout the halite intervals (Raup et al. 1970) and the absence or near-absence of such diagnostic secondary salts as polyhalite and magnesite.

The basin's strong asymmetry with a steeply dipping northeast limb and a gently dipping southwestern limb (Figure 4) bespeaks of its taphrogeosynclinal character. A large displacement normal fault delineated the northeastern margin of the basin from the uplands of the Uncompahgre uplift during Paradox deposition; these uplands were the source of most detritus which entered the basin. In addition, it is probable that land areas far to the southwest contributed lesser quantities of detritus.

Retsof Mine. The Retsof Mine (International Salt Co.) is located along the western margin of the Appalachian Basin at the village of Retsof (York Township, Livingston County) in western New York State about 80 km east of Buffalo (Figure 6). Mine production is from a single 3- to 4-m halite bed, the Retsof salt bed, at the top of the middle member of the Vernon Formation. The Vernon Formation is the basal unit of the Upper Silurian (Cayugan) Salina Group throughout New York and northwestern Pennsylvania (Figure 7). Overlying units of the Salina

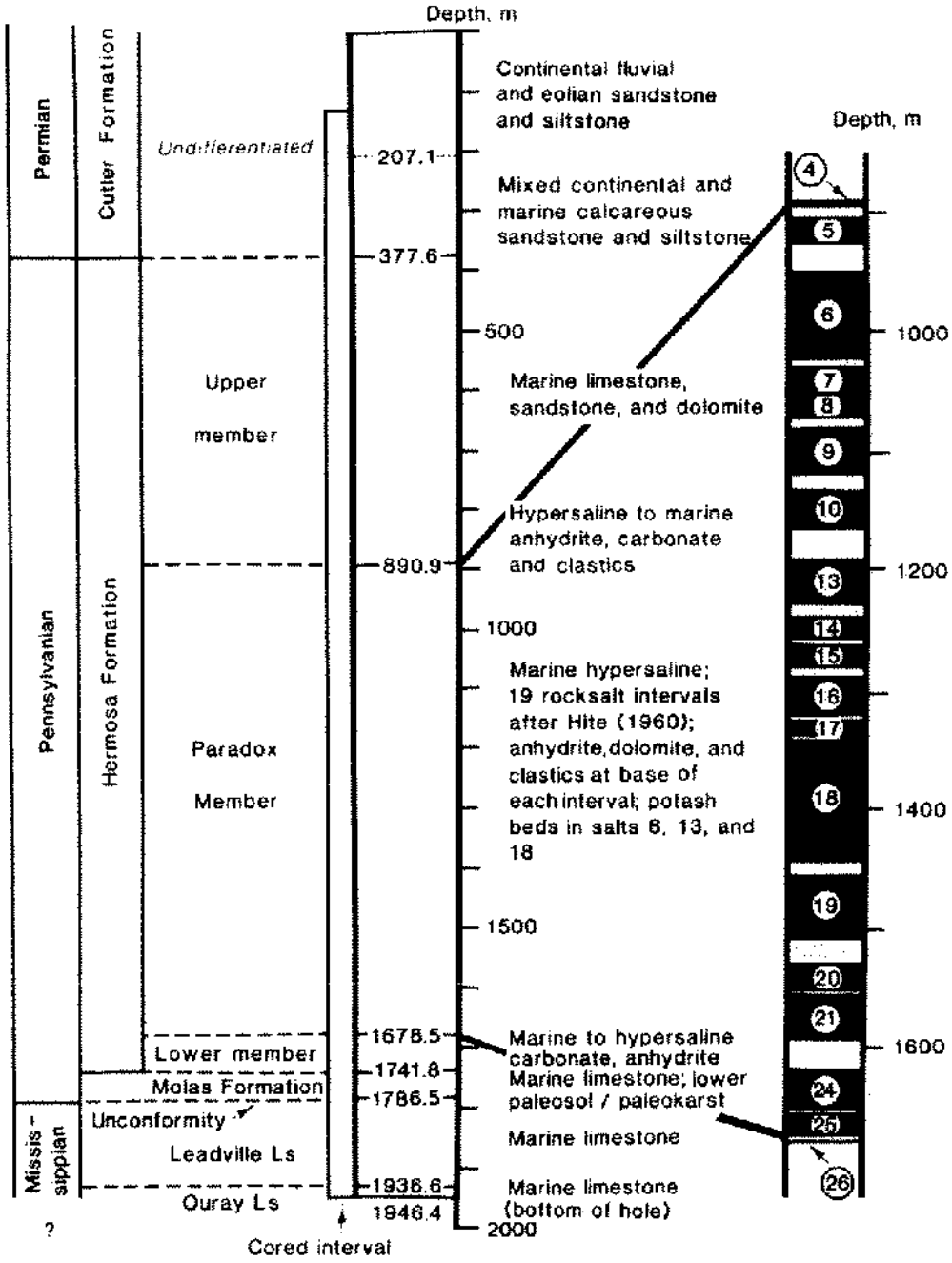

Figure 5. Generalized stratigraphic column in the Gibson Dome No. 1 drill hole, San Juan County, Utah, from Woodward-Clyde (1982) with an expanded section of the Paradox Member with Hite's (1960) numbered salt intervals.

Group in the Retsof area are the Syracuse Formation, the Camillus shale, and the Bertie Formation.

Evaporative concentration in the depositional environments of Salina Group evaporites in western New York State proceeded no further than halite precipitation; dolomite, anhydrite, and halite are common but soluble potash and magnesium salts are absent. Sedimentologic features of the salt at the Retsof Mine have been interpreted by Dellwig and Evans (1969) as originating in relatively shallow water, which, at least some of the time, was above wave base. Pronounced cross-stratification in thicker salt beds, the diffuse character of bedding and banding, the presence of isolated rounded "shale balls," and anhydrite admixed with halite rather than forming

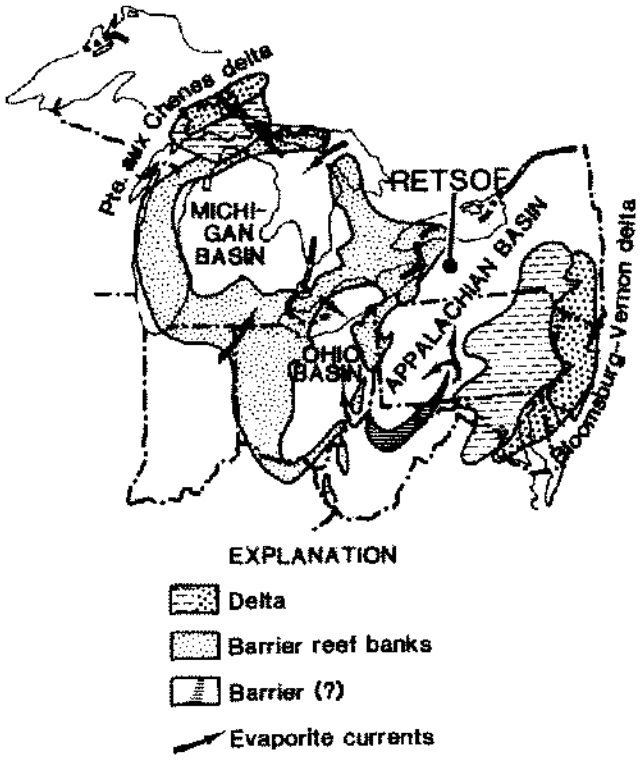

Figure 6. Location map of the Retsof Mine with reconstruction of Cayugan paleogeography showing suggested Niagaran reef banks, delta complexes, and barriers after Alling and Briggs (1961).

sharp anhydrite-halite banding so common in deeper water environments to the west prompted their conclusions that contemporaneous with salt deposition there was considerable remixing of the soft salt "mush."

The salt beds in the Vernon Formation thin rapidly and pinch out to the east with parallel coarsening of the clastic beds which grade into the thick deltaic beds of the Bloomsburg Formation in central and eastern Pennsylvania (Figure 6). To the west, the Retsof salt bed has been traced in the subsurface through northwestern Pennsylvania, northern Ohio, and across the Chatham sag into the Michigan Basin (Rickard, 1969). There is general agreement (Alling and Briggs, 1961; Rickard, 1969) that the principal detrital source for the Vernon Formation lay far to the east in uplands on the eastern margin of the basin (Figure 6); the siliceous detritus in the Retsof area is fine, well weathered material which had a rather lengthy and complex transport history.

Other than dehydration of primary gypsum to anhydrite there is little indication of salt diagenesis, recrystallization, or metasomatism. The bromine contents of halites from Retsof (Dellwig and Evans, 1969; Bodine and Standaert, 1977) indicate an unaltered primary precipitate.

CLAY MINERALOGY AND CHEMISTRY

This report utilizes published and unpublished determinative data for 75 clay separates from the ERDA-9 core (Bodine, 1978), 14 from the Gibson Dome No. 1 core (Bodine and Rueger, in press), and 21 from the Retsof Mine (Bodine and Standaert, 1977). Of these, 57 clay assemblages from the ERDA-9 core, 4 from the Gibson Dome No. 1 core, and 9 from the Retsof Mine have been chemically analyzed. Clay samples from each locality are from representative evaporite lithologies as well as from clastic interbeds. The clay assemblages were separated, fractionated, and analyzed, using, for the most part, standard separation and X-ray determinative procedures (Brindley and Brown, 1980; Carroll, 1973; Grim, 1968).

Clay minerals. Except for illite, the clay minerals from the three localities are trioctahedral and magnesium rich (Table 2). Mg-rich chlorite (clinochlore), regularly interstratified chlorite-trioctahedral smectite (corrensite) to randomly interstratified chlorite-trioctahedral smectite, discrete trioctahedral smectite, interstratified talc and trioctahedral smectite, talc, and serpentine have been identified.

Illite (Table 2) is the only dioctahedral clay occurring in these assemblages. It is extremely well crystallized and appears to contain little, if any interstratified expandable layers. The absence of any low-angle asymmetry in the 001 reflection is attributed by Reynolds (1980) to those illites with substantially less than 10 percent smectite interlayers. Microprobe analysis of illite flakes from the Retsof salt bed (Bodine and Standaert, 1977) yields a structural formula of

$$K_{0.85}(Al_{1.61}Fe^{3+}_{0.20}Mg_{0.23})(Al_{0.76}Si_{3.24})O_{10}(OH)_2$$

which is well within compositional limits for discrete illite (Weaver and Pollard, 1973). Chemical composition of illite-rich assemblages (Table 3, nos. 1a, 1b, 1c) show characteristic high K_2O content when compared with Al_2O_3. Illite occurs throughout samples from each locality, and in numerous samples illite is the dominant mineral in the clay assemblage.

Chlorite (Table 2) is the most aluminous of the trioctahedral clays and occurs at all three localities. It is characteristically well crystallized and yields diagnostic diffraction maxima. The structural formula of the chlorite from the Retsof Mine from electron microprobe data (Bodine and Standaert, 1977) is

$$(Mg_{4.51}Fe^{2+}_{0.23}Al_{1.21})(Al_{1.09}Si_{2.91})O_{10}(OH)_8$$

which falls well within the clinochlore composition for megascopic chlorites (Foster, 1962) and clay chlorites (Bailey, 1982); chemical analyses of chlorite-bearing assemblages are given in Table 3, nos. 1a, 1c, and 5b. Chlo-

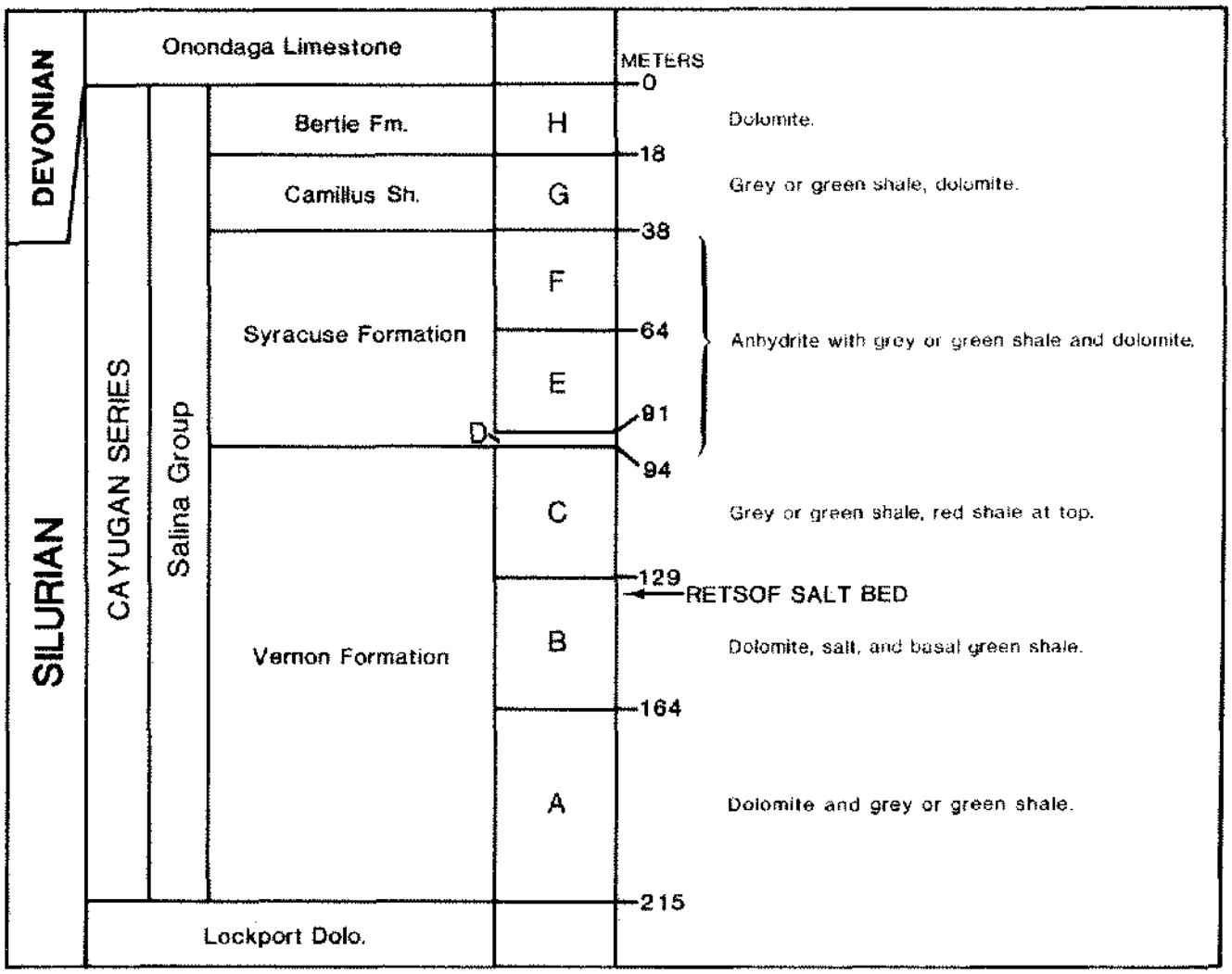

Figure 7. Generalized stratigraphic column of Cayugan rocks in the MacDonald No. 1 drill hole, York Township, Livingston County, New York near the Retsof Mine with lettered intervals representing correlation with the standard Michigan Basin section after Rickard (1969).

rite is the only Al-bearing trioctahedral clay in the Retsof salt bed and dominates many of the clay assemblages. In the Gibson Dome No. 1 core, chlorite is common but is generally less abundant than the interstratified chlorite-trioctahedral smectites. In the ERDA-9 core, chlorite also occurs but neither ubiquitously nor generally abundantly; the smectite-bearing mixed-layer varieties are the dominant trioctahedral Al-bearing species.

Interstratified chlorite and trioctahedral smectite (Table 2) is abundant throughout the ERDA-9 and Gibson Dome No. 1 salts. Three mineral varieties of these interstratified clays form a crystal chemical continuum: (1) corrensite yielding a rational series of sharp superlattice spacings which indicates regularly alternating interstratification and a composition approaching 1:1 chlorite:trioctahedral smectite (Bailey, 1982); (2) a corrensite-like mineral which, like corrensite, yields superlattice diffraction maxima but they deviate somewhat from rationality suggesting some randomness of the interstratification and modest departure from the 1:1 composition; and (3) a mixed-layer clay yielding no superlattice reflections which has highly random interstratification and may vary markedly from the 1:1 composition. Throughout this report the term "corrensite" will be restricted to the first variety, "corrensite-like clay" to the second, and "randomly interstratified chlorite-smectite" to the third.

Corrensite is less aluminous than discrete chlorite because the trioctahedral smectite layer contains at most a fraction of an aluminum ion per formula unit (Table 2). The structural formula of corrensite from an essentially monomineralic sample in the Paradox Member (Table 4) suggests the interlayer cation charge requirement of the

TABLE 2

Clay Minerals Identified in ERDA-9, Gibson Dome No. 1, and Retsof Mine Evaporites and Intercalated Clastics

Clay Mineral	Generalized Chemical Formula	Al_2O_3 (wt. %)
Illite	$K_{0.85}(Al_{1.6}Fe^{3+}_{0.2}Mg_{0.2})(Si_{3.35}Al_{0.65})O_{10}(OH_2)$	~28
Chlorite	$([Mg,Fe]_5Al)(Si_3Al)O_{10}(OH)_8$	~18
Interstratified chlorite-trioctahedral smectites		
Corrensite	$(chlorite)_{0.5}(trioctahedral\ smectite)_{0.5}$	~12
Corrensite-like	$(chlorite)_{\sim 0.5}(trioctahedral\ smectite)_{1-\sim 0.5}$	~12
Random	$(chlorite)_x(trioctahedral\ smectite)_{1-x}$	~5–15
Trioctahedral smectite	$M^{0.33+}_{ex.}Mg_3(Si_{3.67}Al_{0.33})O_{10}(OH)_2$	~2–4
Interstratified talc-trioctahedral smectite	$(talc)_x(trioctahedral\ smectite)_{1-x}$	<3
Talc	$Mg_3Si_4O_{10}(OH)_2$	0
Serpentine	$Mg_3Si_2O_5(OH)_4$	0

$M^{0.33+}_{ex.}$ — Charge contribution by cations in exchangeable sites.

TABLE 3

Chemical Analysis (weight percent) of Clay Fractions (<2 μm) from ERDA-9, Gibson Dome No. 1, and Retsof Mine Evaporites and Intercalated Clastics

	1a	1b	1c	2a	2b	2c	2d	3a	4a	4b	5a	5b	6a	6b
SiO_2	60.4	46.3	47.2	52.0	47.7	39.0	42.9	47.6	54.4	57.7	52.6	46.7	43.2	45.4
TiO_2	0.81	0.44	0.48	0.90	0.64	0.37	0.15	0.40	0.20	0.28	0.09	0.26	0.11	0.43
Al_2O_3	14.3	12.1	20.1	12.36	9.54	12.5	9.31	7.83	3.80	5.84	2.38	7.97	3.15	6.56
Fe_2O_3*	5.29	11.47	3.57	2.20	1.36	4.40	2.00	3.14	3.76	9.17	0.35	6.84	1.24	12.18
MnO	0.07	nd	<0.02	nd	nd	<0.02	<0.02	nd	nd	nd	nd	0.05	nd	0.05
MgO	5.67	20.7	11.6	23.6	28.6	26.5	30.7	23.5	27.7	22.6	27.4	21.4	38.8	15.6
CaO	0.14	0.09	0.60	0.06	0.06	0.07	<0.02	0.73	0.09	0.12	0.08	0.12	0.03	0.32
Na_2O	0.30	0.58	0.28	0.85	1.01	0.97	0.79	2.15	0.35	0.44	1.56	0.18	1.04	0.34
K_2O	3.82	3.55	5.37	2.21	1.86	0.87	0.11	2.10	0.56	0.97	0.41	0.45	<0.02	0.89
P_2O_5	0.05	nd	0.20	nd	nd	0.38	<0.05	nd	nd	nd	nd	0.03	nd	0.05
S	1.10	nd	nd	nd	nd	nd	nd	nd	nd	nd	nd	3.13	nd	6.73
LOI†	nd	nd	10.1	nd	nd	13.6	13.2	nd	nd	nd	nd	nd	nd	nd

1. Illite-rich assemblages.
   a. RS-72-20, Retsof Mine, uppermost Retsof salt bed: ill=chl>tal with quartz and minor pyrite.
   b. JL-CS-11, ERDA-9, McNutt potash zone polyhalite: ill=rcs>chl with hematite.
   c. GD1-15, Gibson Dome No. 1, Paradox cycle 19 anhydrite: ill>chl (Bodine and Rueger, in press).
2. Interstratified chlorite-trioctahedral smectite-rich assemblages.
   a. MB-CS-21, ERDA-9, McNutt potash zone rock salt: rcs>ill=tal>chl.
   b. JL-CS-14, ERDA-9, McNutt potash zone claystone: cor≫ill.
   c. GD1-7, Gibson Dome No. 1, Paradox cycle 5 siltstone: cor≫ill=chl (Bodine and Rueger, in press).
   d. GD1-11, Gibson Dome No. 1, Paradox cycle 6 rock salt: cor≫ill=tal (Bodine and Rueger, in press).
3. Trioctahedral smectite-rich assemblage.
   a. MB-CS-13, ERDA-9, lower Salado anhydrite: tsm>ill>chl.
4. Interstratified talc-trioctahedral smectite-rich assemblages.
   a. JL-CS-19, ERDA-9, McNutt potash zone polyhalite: tts≫ill.
   b. JL-CS-23, ERDA-9, upper Salado polyhalite: tts≫ill with hematite.
5. Talc-rich assemblages.
   a. MB-CS-15, ERDA-9, lowermost Salado anhydrite: tal≫tsm>ill.
   b. RS-72-5, Retsof Mine, middle Retsof salt bed: tal=chl≫ill.
6. Serpentine-bearing assemblages.
   a. MR-CS-42, uppermost Castile anhydrite: ser>tsm>chl.
   b. RS-72-11, Retsof Mine, lower Retsof salt bed: tal≫chl=ser=ill with pyrite.

Mineral abbreviations: chl—chlorite; cor—corrensite or corrensite-like clay; ill—illite; rcs—randomly interstratified chlorite-trioctahedral smectite; ser—serpentine; tal—talc; tsm—trioctahedral smectite; tts—interstratified talc—trioctahedral smectite.

Analysts: ERDA-9 samples—John Laskin, New Mexico Institute of Mining and Technology; Gibson Dome No. 1 samples—Analytical Laboratories (Denver), U.S. Geological Survey; Retsof Mine samples—Max Budd, S.U.N.Y. Binghamton.

*Total iron as Fe_2O_3.

†Loss on ignition at 900°C.

nd Not determined.

TABLE 4

Structural Formula of Corrensite from the Paradox Formation [calculated from chemical analysis of GD1-11 < 1 μm fraction (table 3; no. 2d) for 25 oxygens (14 in chlorite, 11 in smectite) with iron as FeO]

Tetrahedral:*	Si^{4+}	7.12
	Al^{3+}	.88
Total		8.00
Octahedral:†	Al^{3+}	.95
	Ti^{4-}	.02
	Fe^{2-}	.25
	Mg^{2+}	7.59
Total		8.81
Interlayer:‡	Na^{+}	.26
	K^{+}	.02
Total		0.28
Tetrahedral charge deficiency:	−0.88	
Octahedral charge excess:	+0.61	
Interlayer charge excess:	+0.28	

*Two sites in each of four sheets: two sheets in smectite 2:1 layer; two sheets in chlorite 2:1 layer.

†Three sites in each of three sheets: one sheet in smectite 2:1 layer; one sheet in chlorite 2:1 layer; one sheet in chlorite brucite-like sheet.

‡Smectite interlayer sites.

smectite layer is satisfied to a large extent by vacancies in octahedral sites, that is, stevensite-like layers, rather than by aluminum substitution for silicon in tetrahedral sites, that is, saponite-like layers. Chemical analysis of assemblages containing abundant interstratified chlorite-trioctahedral smectite (Table 3; nos. 2a, 2b, 2c, and 2d) illustrate the low alumina and high magnesia in these clays.

Interstratified chlorite-trioctahedral smectites are abundant in the Paradox Member from the Gibson Dome No. 1 core (Figure 5); corrensite and corrensite-like clay are the common varieties and the randomly interstratified clay is rare. In the Salado Formation from the ERDA-9 core (Figure 3), corrensite and corrensite-like clay are abundant in the claystone interbeds and also occur, but less frequently, throughout the evaporite lithologies. Conversely the randomly interstratified variety is abundant throughout the evaporite beds and less common in the claystone interbeds. Only negligible amounts of interstratified chlorite-trioctahedral smectite occur in the uppermost Castile Formation.

Discrete Mg-rich trioctahedral smectite (Table 2) also occurs in some assemblages and coexists with variable quantities of other trioctahedral clays and illite. The aluminum-poor character of the discrete smectite is illustrated by the analysis of a smectite-rich assemblage from the McNutt potash zone in the ERDA-9 core (Table 3; no. 3a); much of the Al_2O_3 is present in coexisting illite as indicated by the assemblage's K_2O content. Discrete smectite occurs most commonly, sometimes abundantly, in evaporite beds of the Salado and uppermost Castile Formations from the ERDA-9 core. It is only rarely observed in clay assemblages from the Paradox Member at Gibson Dome No. 1 and is absent in salts from the Retsof Mine.

Interstratified talc-trioctahedral smectite (Table 2) is identified only from the ERDA-9 core. The mineral is less aluminous than the interstratified chlorite-smectite as shown by analyses 4a and 4b of a talc-trioctahedral smectite-rich assemblage (Table 3); again a substantial fraction of the Al_2O_3 in the assemblage is contained in the small quantity of coexisting illite. The mixed-layer talc-smectite is restricted to some polyhalite and adjacent anhydrite beds within or stratigraphically close to the McNutt potash zone. At the same time, other polyhalite and anhydrite beds contain the characteristic Salado Formation clay assemblage of interstratified chlorite-trioctahedral smectite and discrete illite with or without discrete talc.

Discrete talc (Table 2) is common throughout these evaporites and generally coexists with illite and one or more of the trioctahedral Al-bearing clays. A chemical analysis of a talc-rich clay assemblage with chlorite and illite from a Retsof Mine salt (Table 3; no. 5b) illustrates the unusually low Al_2O_3 content of this assemblage. In the Gibson Dome No. 1 and ERDA-9 cores, talc most frequently and abundantly occurs in halite rocks. In the former talc is not found in anhydrites, dolomites, and black shales of the Paradox Member; in the latter talc is occasionally present in anhydrites of the Salado (Table 3, no. 5a) and uppermost Castile Formations and more rarely in polyhalites and claystones of the Salado Formation.

Serpentine (Table 2) is frequently difficult to identify conclusively in these assemblages because of interference of its diffraction maxima with the basal reflections of chlorite. Its uniquivocal occurrence in some Retsof Mine salts and ERDA-9 salts and anhydrites, has been documented (Bodine and Standaert, 1977; Bodine, 1978). Serpentine has not been observed in the Gibson Dome No. 1 core. In the ERDA-9 evaporites, serpentine occurs in several clay assemblages from the uppermost Castile Formation anhydrites and in intercalated halites and anhydrites from the lowermost Salado Formation. In one clay assemblage from the Castile anhydrite, serpentine is the dominant clay and coexists with discrete trioctahedral smectite and minor illite; chemical analysis of the assemblage (Table 3; no. 6a) yields an expected very low Al_2O_3 content. In the Retsof salt bed, the serpentine, never in great abundance, is restricted to the lower part of the bed (Figure 8) and coexists with chlorite, illite, and talc (Table 3; no. 6b). Bromine profiles through the Retsof salt bed show an irregular increase in the bromine content of halite from 75–85 ppm at the base of the bed to 107 ppm at the top (Figure 8). The four serpentine-bearing assemblages are associated with halites containing less than 85 ppm bromine. Based on the stratigraphic relations of serpentine occurrence at both localities as well as bromine data from Retsof, it appears that serpentine is restricted to

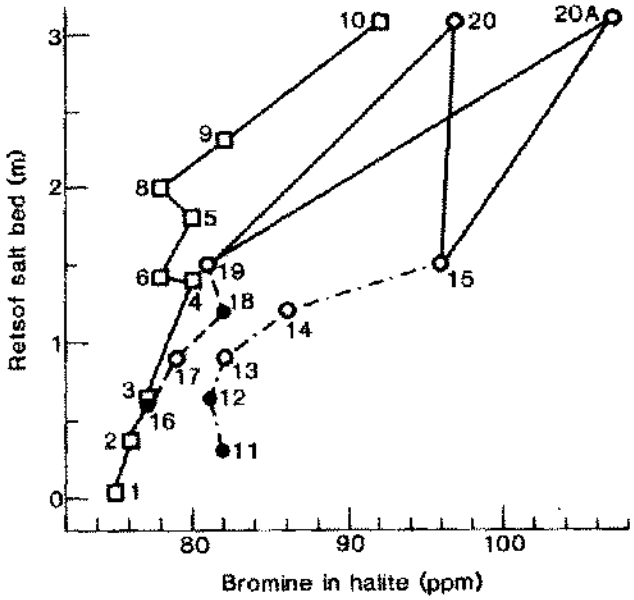

Figure 8. Variation of bromine content (ppm) in halite through the Retsof salt bed from the Retsof Mine: ○ samples with no detectable serpentine and ● samples containing serpentine from two profiles 15 m apart in 4-West (uppermost samples, 20 and 20A, collected from the back between the two profiles); □ samples with no detectable serpentine from 5-West profile.

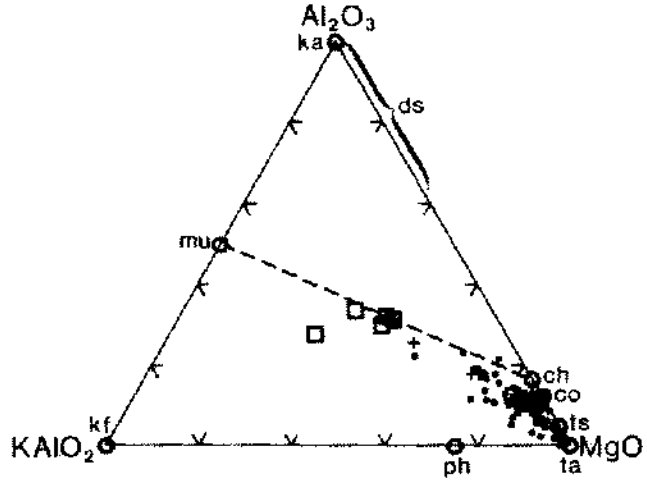

Figure 9. Molar proportions in clay-size residues plotted on the Al_2O_3—$KalO_2$—MgO ternary projection of the Al_2O_3—$KalO_2$—$NaalO_2$—MgO—SiO_2—H_2O system from Salado and uppermost Castile Formations in ERDA-9, ●; the Paradox Member of the Hermosa Formation in Gibson Dome No. 1, +; and the Retsof salt bed in the Retsof Mine, □. Abbreviations for idealized mineral compositions: ch—chlorite (clinochlore); co—corrensite; ds—dioctahedral smectite (montmorillonite-beidellite series); ka—kaolinite, pyrophyllite; kf—potash feldspar; mu—muscovite; ph—phlogopite; ta—talc, serpentine, stevensite; ts—trioctahedral smectite (saponite).

evaporites which precipitated at or near reaching halite saturation during progressive evaporation of the host brine.

Clay mineral associations. Clay mineral assemblages from the three localities have chemistries which fall within a relatively narrow compositional range. On Figure 9, chemical compositions of the clay mineral assemblages have been plotted on the Al_2O_3-$KA1O_2$-MgO three-component projection of the Al_2O_3-$KA1O_2$-$NaAlO_2$-MgO-SiO_2-H_2O system. The compositions of idealized selected sedimentary silicates, shown as open circles, and the tie line between muscovite and clinochlore are plotted for reference. Clay assemblages from these three evaporites cluster very tightly along and below the muscovite-clinochlore tie line. Those compositions below the tie line reflect aluminum depletion due to the presence of talc, discrete and interstratified trioctahedral smectite, and, in a few cases, serpentine.

The distribution of clay minerals in assemblages from the three localities is summarized in Table 5 which illustrates four distinctive features of the assemblages and their associations with evaporite lithologies.

1. Illite is the only dioctahedral clay in these assemblages. It is characteristically well crystallized and contains no recognizable interstratified smectite. Illite occurs ubiquitously in all evaporite lithologies as well as in intercalated clastics. It almost always coexists with either chlorite or an interstratified chlorite-trioctahedral smectite, or both. Frequently talc, and more rarely, serpentine, discrete trioctahedral smectite, or interstratified talc-trioctahedral smectite may also occur with illite.
2. The chlorite at the three localities is an Mg-rich clinochlore. It is abundant and the sole Al-bearing trioctahedral clay in clay mineral assemblages from the Retsof Mine salt. It also occurs in all lithologies in the Paradox Member from the Gibson Dome No. 1 core but characteristically coexists with more abundant corrensite or corrensite-like mixed-layer clays. In the ERDA-9 core, the interstratified chlorite-trioctahedral smectite clays dominate the Salado Formation; chlorite does occur in many assemblages, but generally it is not abundant. Randomly interstratified chlorite-trioctahedral smectite is abundant in ERDA-9 assemblages from halites and progressively less abundant in anhydrites, polyhalites, and claystones; corrensite and corrensite-like clay dominate assemblages from claystones, some anhydrites and polyhalites, and rarely halites.
3. Interstratified talc-trioctahedral smectite occurs only in the ERDA-9 core. There it is restricted to some polyhalite and fewer adjacent anhydrite beds which occur in or stratigraphically close to the

McNutt potash zone (Figure 3). In several clay mineral assemblages, it is essentially monomineralic, and the interstratified chlorite-trioctahedral smectite clays are absent; in some the interstratified talc-smectite does coexist with a chlorite-bearing mixed-layer clay. In other polyhalite and related anhydrite beds, on the other hand, the clay minerals consist of the more normal assemblage with abundant interstratified chlorite-trioctahedral smectite and no interstratified talc-trioctahedral smectite.

4. Talc is widely distributed and occasionally abundant among evaporite lithologies at the three localities. It is particularly abundant in most clay mineral assemblages from the halite intervals of the Paradox Member in the Gibson Dome No. 1 core and in rock salt at the Retsof Mine. Talc in the ERDA-9 core occurs sporadically in all lithologies of the Salado and uppermost Castile Formations. Serpentine, on the other hand, occurs in clay mineral assemblages from the Retsof Mine and the ERDA-9 core, but in each case is restricted to those evaporites which precipitated from brines which were at or near halite saturation during progressive evaporative concentration.

DISCUSSION

The uniformly distinctive chemical and mineralogic character of clay mineral assemblages from the three evaporite localities parallels the equally distinctive character of the three depositional environments. The role that the marine hypersaline environment played in the genesis of these clays through Mg-metasomatism of average aluminous detritus is the principal conclusion of this report. In addition, there are specific mineralogic features of the clay mineral assemblages which prompt two somewhat more speculative interpretations: conditions of talc and serpentine deposition, and the origin of interstratified talc-trioctahedral smectite.

Mg-metasomatism. Millot (1970) clearly recognized the importance of the depositional environment when he concluded that many clays in hypersaline rocks are authigenic. Yet other investigators, such as Droste (1963) and Lounsbury (1963), have attributed the origin of the clays chiefly to provenance and burial metamorphism with negligible or minor contribution from the hypersaline environment. A recent example of the latter view is given by Register (1981) when he states that in the Salado Formation "the clay mineralogy suggests that a significant amount of the clay minerals found in evaporite rocks are detrital and not authigenic."

Clay mineral assemblages from this study strongly support Millot's (1970) conclusions. Interaction between the marine hypersaline environment and "average" aluminous detritus appears to have been the principal factor in the formation of these clay mineral assemblages.

The region on the Al_2O_3-$KAlO_2$-MgO projection occupied by the composition of clay assemblages from the three localities is outlined on Figure 10; the data points of Figure 9 have been omitted. Also plotted are examples of shale and clay compositions in normal marine and continental strata and two shale-composition averages, as well as compositions of clay fractions from the German Zechstein (Niemann, 1960) and Keuper (Echle, 1961) evaporites. The composition of the German hypersaline clays clearly falls within the delineated region. However, the clay and shale compositions from normal marine and continental rocks fall outside the region; they are substantially less magnesian and more aluminous. It might be argued that clay assemblages from a single evaporite sequence might have such distinctive composition through some unusual character of the source area or some post-depositional deep burial process but these data include clay mineral assemblages from five evaporite deposits representing five different source terrains, five different basins with five different diagenetic and burial histories, and a range of geologic ages from the Silurian to the Triassic. The tight cluster of compositions for evaporite clays from five localities, their isolation from normal marine,

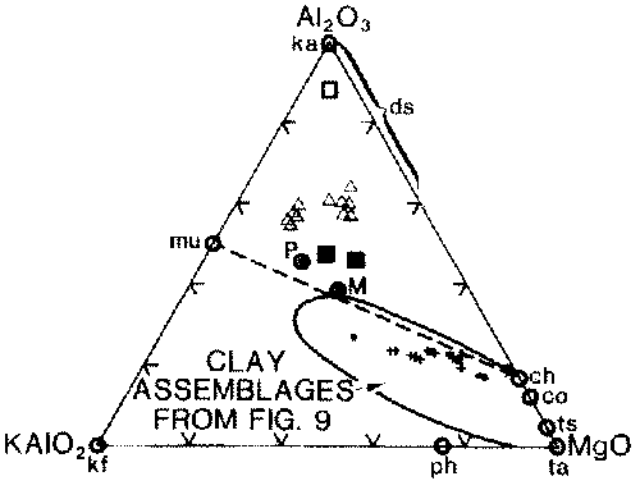

Figure 10. Molar proportions of silicate assemblages plotted on the Al_2O_3—$KalO_2$—MgO ternary projection of the Al_2O_3—$KalO_2$—$NaAlO_2$—MgO—SiO_2—H_2O system. Clay fractions from other marine evaporite sections: the Zechstein Craven Salzton (grey claystone) from the "Königshall-hindenburg" Mine near Göttingen, West Germany, + (Niemann, 1960); and carbonate strata from the German Keuper near Göttingen, ● (Echle, 1961). Clay fractions from normal marine and continental strata: paleosol in lowermost Molas Formation, □, and marine shales from the Molas Formation, ■, from Gibson Dome No. 1 drill hole, Utah (Bodine and Rueger, in press); and from Gulf Coast Tertiary shales, Δ (Hower and others, 1976). Average shale composition (whole rock) compiled in Pettijohn (1975), with P for Paleozoic and M for Mesozoic. Heavy boundary represents area of diagram occupied by clay assemblage compositions form this study (fig. 9); abbreviation of idealized mineral compositions from figure 9.

continental, and average clay compositions, and the compatibility between their anomalous chemistry and the unusual chemistry of their depositional environment strongly suggest there was extensive interaction between argillaceous detritus accumulating in the basin and the coexisting host brines with enhanced magnesium and potassium concentrations.

Mineralogic characteristics in these assemblages further support the conclusion. Talc is common in these assemblages and very abundant in many. It occurs at all three deposits (Table 5), in the German Zechstein (Braitsch, 1971), and in other marine salt deposits (Millot, 1970). Yet it is only rarely observed, and then not abundantly, in clay mineral assemblages of nonevaporite sedimentary strata (Friedman, 1965). Corrensite is also an abundant and ubiquitous mineral in many salt deposits (Table 5) but is infrequently abundant in other sedimentary rocks (for example, Peterson, 1961). Illites in the evaporites are uniformly well crystallized and contain negligible smectite interlayers while most sedimentary illites show at least some recognizable mixed layering (Reynolds, 1980). The illite in the Retsof clay mineral assemblages contains 0.85 interlayer potassium ions per structural formula unit (Bodine and Standaert, 1977) while ideal endmember sedimentary illite is suggested to contain 0.60–0.80 potassiums per structural formula unit (Helgeson and Mackenzie, 1970; Perry, 1971). Chlorites from the Retsof Mine clay assemblages (Bodine and Standaert, 1977) and the Königshall-Hindenburg potash mine salt clay in the German Zechstein (Niemann, 1960) have Fe:Mg atom ratios under 0.1; in shale chlorites the ratio characteristically exceeds 0.3 and commonly 0.5 (Weaver and Pollard, 1973). Any one of these mineralogic features is not necessarily persuasive of an authigenic origin. Collectively their pervasive occurrence in marine evaporite clay mineral assemblages and their anomalous character when compared with average clay detritus strongly suggest the importance of interaction with the hypersaline environment in their formation.

Clay minerals from geologically active or very young depositional environments provide evidence of incipient Mg-metasomatism by natural waters. In alkaline Lake Abert, Oregon, for example, Jones and Weir (in press) document Mg-enrichment of detrital smectites. The dioctahedral smectite with some chloritic intergrades which formed from weathering volcanics becomes transformed in the saline lake bottom muds into an Mg-enriched smectite with octahedral site occupancy of 2.4–2.5 and noticeably more chloritic intergrades. Jones and Weir also suggest, although without conclusive evidence, that domains of illite are forming in some smectites in the very fine size fraction of the bottom muds. Eberl et al. (1982) and Khoury et al. (1982) have described Plio-Pleistocene neoformation of sepiolite and its transformation to a kero-

TABLE 5

Occurrence of Clay Minerals in ERDA-9, Gibson Dome No. 1, and Retsof Mine Evaporites and Intercalated Clastics

	ERDA-9	GD-1	Retsof	
Illite	XXX	XXX	XXX	Ubiquitous
Chlorite	X	XX	XXX	Nearly ubiquitous
Interstratified chlorite-trioctahedral smectite				
Corrensite and/or corrensite-like slay	Xo	XXo	—	Absent at Retsof
Random	XX	X	—	Absent at Retsof
Trioctahedral smectite	XX	o	—	Absent at Retsof
Interstratified talc-trioctahedral smectite	ooo	—	—	Some ERDA-9 polyhalites and associated anhydrites only
Talc	Xoo	XXo	XXo	Uncommon in clastics and carbonates
Serpentine	oo	—	oo	Some anhydrite/halites at/near first halite precipitation

Little or no stratigraphic/lithologic restriction.
X Present but not common nor abundant
XX Moderately common and/or abundant
XXX Common and frequently abundant
Substantial stratigraphic/lithologic restriction.
o Present but not common not abundant
oo Moderately common and/or abundant
ooo Common and frequently abundant

lite-stevensite mixed layer clay through interaction between volcanic glass detritus in a high dissolved silica, alkaline lacustrine environment from the Amargosa Desert, Nevada. Bodine (1971) reported neoformed talc and Mg-enrichment of smectites in modern bottom sediments of the Grote Zoutpan, St. Maarten, Lesser Antilles; the coexisting marine hypersaline brine is commonly halite saturated and has a very low dissolved silica content (0.5 ppm).

In the Paleozoic evaporites, these processes apparently continued to completion where, in addition to interaction between argillaceous detritus and hypersaline brines in the depositional environment, there was continued interaction with coexisting entrapped brine during early diagenesis followed by time-dependent internal ordering reactions with or without increased temperatures which produced the well crystallized clay minerals observed in these rocks.

Talc and serpentine. The occurrence of talc and serpentine in the Retsof Mine and ERDA-9 salts can be related to their respective equilibria in the MgO-SiO_2-H_2O system. The system has most recently been examined by Hemley and others (1977) and their results (Figure 11) show a progression of mineral stabilities from quartz, through talc, then serpentine, and finally brucite as functions of increasing $Mg^{+2}/(H^+)^2$ ion activity ratio and decreasing dissolved silica (H_4SiO_4) activity in the coexisting aqueous solution. Serpentine stability requires a brine with higher $Mg^{+2}/(H^+)^2$ activity ratio than does talc stability.

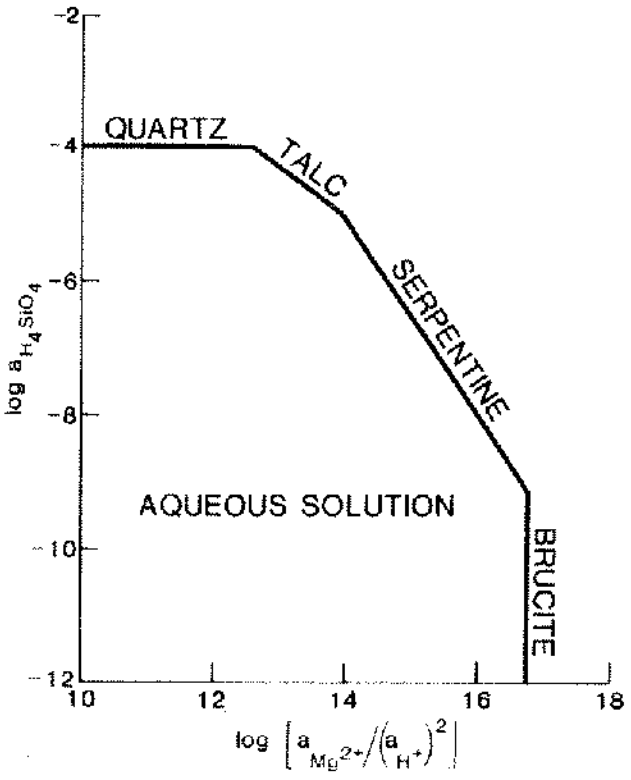

Figure 11. Stability relations in the system MgO—SiO_2—H_2O at 25°C and 1 atm pressure as function of H_4SiO_4 activity and $Mg^{2+}/(H^+)^2$ activity ratio in the coexisting aqueous fluid; modified from Hemley and others (1977).

The most straightforward mechanism of increasing the ion activity ratio is by progressive evaporative concentration of the magnesium at constant pH. However, under these conditions it would be expected that serpentine stability would be reached late in the marine salt progression and would continue with further evaporation. This is not the case. Observations at the Retsof Mine and in the ERDA-9 core indicate that serpentine is restricted to a limited interval in the marine salt progression where halite saturation is initially attained. Salts precipitated from both more dilute brines earlier in the progression and more concentrated brines later in the progression commonly contain abndant talc but no serpentine.

The hydrogen ion activity, or pH, remains as the alternative variable. Herrmann and others (1973) reported systematic pH decline with evaporative concentration in the more concentrated brines of Adriatic waters at the solar salt facility in Portoroz, Yugoslavia. They measured pH's of 8.1–8.3 from initial seawater into brines precipitating calcium sulfate ($d = 1.106$ g/cm^3). From more concentrated brines precipitating calcium sulfate ($d = 1.212$ g/cm^3) into active halite-producing brines ($d = 1.248$ g/cm^3) the pH progressively declined from 7.62 to 6.57. Bodine (1976) has suggested that prior to halite saturation very small quantities of a magnesium hydroxychloride salt begin to precipitate which results in a systematic pH decrease with increasing magnesium activity such that pH < 5 is likely in Mg-rich bitterns. The pH's recorded in brine seeps from the Salado Formation in the Duval potash mine are 5.4–5.5 (Lambert, 1978), and in brines collected from the Paradox Member of the Hermosa Formation in southeastern Utah, which are believed to be modified connate brines, the pH's (Table 6) are as low as 4.0 (O. B. Raup, written commun.).

Suggested variations of pH and magnesium activity in the hypersaline fluid as a function of the precipitating marine salt progression are shown schematically on Figure 12. Activity values for magnesium cannot be rigorously assigned because of high ionic strengths of marine bitterns. Although magnesium ion activity does increase throughout the progression, the onset of declining pH during calcium sulfate precipitation causes a maximum of the $Mg^{+2}/(H^+)^2$ ion activity ratio to occur in the vicinity of initial halite saturation (Figure 12). It is within this region of the progression where serpentine would most likely be the stable magnesium silicate; on either side of this maximum talc would be the stable phase. This model conforms remarkably well with serpentine distribution in Retsof Mine and ERDA-9 salts.

Thus, the speculative suggestion is offered that serpen-

TABLE 6

Chemical Analysis (mg/kg except for pH and density) of Brines from the Paradox Member of the Hermosa Formation in Southeastern Utah from O. B. Raup (written commun.)
[nd—not determined]

	1	2	3	4
Ca	41,300	56,200	32,300	132,000
Mg	30,200	25,200	27,800	6,720
Na	13,300	18,500	22,200	6,650
K	36,500	15,000	36,700	17,800
Cl	227,000	215,000	208,000	288,000
Br	nd	nd	1,600	2,360
HCO_3	<600	<600	nd	<1
SO_4	<100	<100	100	<1
Density (g/cm^3)	1.350	1.282	1.282	1.444
pH	4.45	4.8	4.8	4.0

1. Sample B-2, "black oil zone" of Paradox salt, Murphy Corporation No. 1 Federal well, Grand County, Utah; Analyst, U.S. Geological Survey Analytical Laboratories, Denver (1965).
2. Sample B-3, "Cane Creek Marker" of Paradox salt, Modco M.G.M. No. 2 well, Grand County, Utah; Analyst, U.S. Geological Survey Analytical Laboratories, Denver (1965).
3. Sample B-4, Salt bed 16 of Paradox Member, White Clout No. 2 well, Grand County, Utah; Analyst, U.S. Geological Survey Analytical Laboratories, Denver (1965).
4. Gas bleeder drill hole into base of cycle 4 of Paradox Member in Texas Gulf Sulfur Co. potash mine near Moab, Utah; Analyst, Shirley Retig, U.S. Geological Survey, Water Resources Division, Reston (1968).

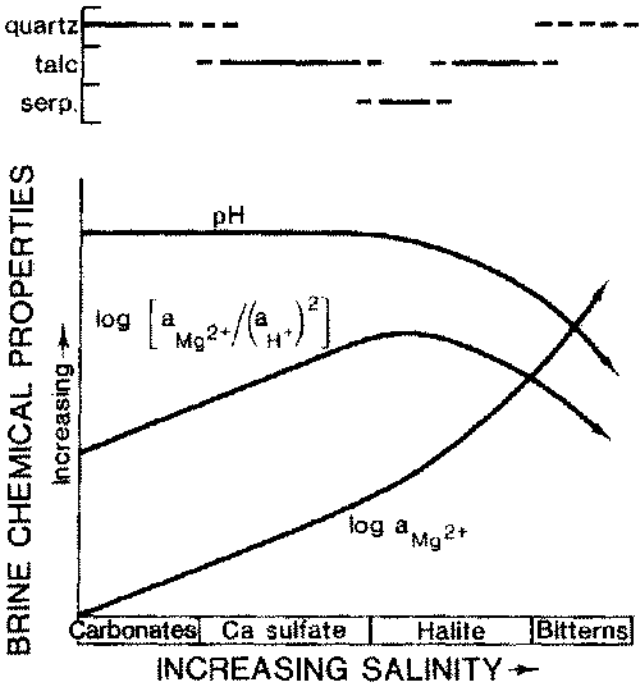

Figure 12. Suggested schematic relations between chemical properties of marine evaporite brines and mineral stabilities within the $MgO—SiO_2—H_2O$ system during progressive evaporation of seawater.

tine and much-to-most of the talc in these evaporites crystallized as neoformed silicates in the hypersaline depositional or earliest postdepositional environments and their speciation reflects magnesium activity and pH variation in the coexisting brine.

Clays in polyhalite. The clay mineralogy in several polyhalite and adjacent anhydrite beds from the Salado Formation of the ERDA-9 core is unusual. Instead of the characteristic interstratified chlorite-smectite dominating the clay mineral assemblage, an interstratified talc-trioctahedral smectite is the abundant clay mineral. This talc-bearing clay is markedly Al-depleted (Table 3; 3a, 5a). The origin of the Al-depleted assemblage may be attributed to either depositional or diagenetic processes.

A depositional origin would require that either the character of the detrital influx entering the basin, or the character of the interaction between the detritus and the host brine changed periodically and markedly. Because there is general agreement that polyhalite in the Salado Formation is secondary and diagenetically replaced primary calcium sulfate precipitates, it becomes unrealistic to propose that either depositional perturbation would occur only during episodes of calcium sulfate deposition in which subsequent diagenesis would alter the calcium sulfate to polyhalite.

Alternatively a diagenetic origin requires replacement of the characteristic Al-bearing chloritic clay assemblage by the Al-depleted talc-bearing assemblage. This could be accomplished either by conservation of alumina and massive addition of magnesium and silica to the clay fraction, or by leaching aluminum from the clays with negligible gain or loss of magnesium and silica.

Conservation of aluminum appears distinctly more attractive because of the low solubility of aluminum in most natural waters. However, two features of the altered and unaltered clays suggest that it is unlikely that aluminum was conserved during the clay alteration process.

First, conserving aluminum and, at the same time, severely reducing its relative abundance in the insoluble residue (chiefly the clay minerals) from 10–13 to 2–4 weight percent Al_2O_3 (Table 3; 3c and 5a) would require massive additions of magnesium and silica; this would have increased the total clay in the host evaporite by at least a factor of three or four. No such increase is observed. Insoluble residue abundances in 11 sulfate rocks with Al-bearing clays range from 0.18 to 1.10 weight percent with a mean of 0.6 weight percent; the abundances in nine sulfate rocks with Al-depleted clays range from 0.14 to 0.85 weight percent with a mean of 0.4 weight percent. If the differences in residue abundances between the two populations were significant, it is the reverse of that expected were aluminium conservative.

Second, if magnesium and silica were added to the insoluble fraction, their abundances relative to another component other than aluminum should be diagnostic.

Magnesium or silica ratios with total iron show no such segregation of the two populations (Figure 13a) although a clear segregation of the two populations exists for the magnesium or silica ratios with alumina (Figure 13b). Were alumina conserved the segregation of the two populations should be equally pronounced in each diagram unless there were the very unlikely coincidence that iron enrichment paralleled that of silica and magnesium during the transformation reaction.

The comparison of residue abundances and compositional ratios between the two populations are entirely consistent with an Al-leaching hypothesis. That alternative, however, requires unusual chemical properties of the alteration pore fluids. Not only must a high magnesium activity be maintained to assure stability of the Mg-rich clays, but extreme pH is required if aluminum is to be leached from the chloritic layers.

Because the Al-depleted clays are restricted to some polyhalite and adjacent anhydrite beds, it appears reasonable to assume that the clay transformation was contemporaneous with replacement of the primary calcium sulfate by polyhalite. Not only must the sulfate reaction have required brine mobility with appropriately high Mg-concentration in the brine, but the replacement process itself would have effectively exposed the silicates to the fluid phase rather than leaving them isolated in a closed system as inclusions in inert salts.

Another assumption is that these fluids were most likely strongly concentrated brines which closely resembled, and possibly evolved from surficial evaporative bitterns. In such brines, the activity of water would have been markedly reduced. Water vapor pressure measurements for the marine salt system, compiled in Stewart (1963), yield water activities of 0.51, 0.40, and 0.31 in brines at the hexahydrite-kieserite-kainite-halite, the kainite-kieserite-carnallite-halite, and the bischofite-kieserite-carnallite-halite invariant points respectively.

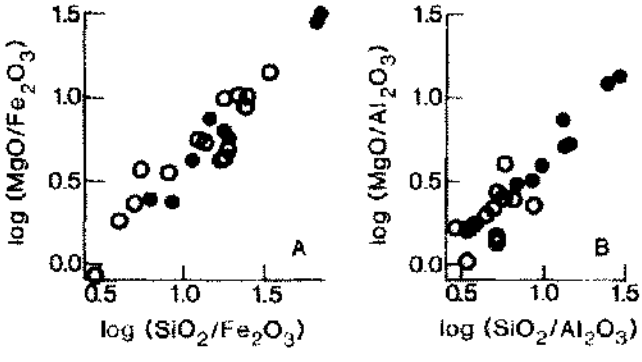

Figure 13. Oxide weight percent ratios in clay-size residues in sulfate rocks from the Salado Formation in ERDA-9 core: A. log (MgO/Fe_2O_3) *vs* log (SiO_2/Fe_2O_3); B. log (MgO/Al_2O_3) *vs* log (SiO_2/Al_2O_3). Total iron expressed as Fe_2O_3. Character of dominant clay mineral: ● interstratified talc-trioctahedral smectite; ○ interstratified chlorite-trioctahedral smectite.

Finally, as discussed in the preceding section, there is evidence that the pH of marine bitterns and pore fluids evolved from marine bitterns is characteristically unusually low. It then appears reasonable to assume that the bittern pore fluids responsible for the sulfate replacement and accompanying clay mineral reactions were acidic, most likely strongly acidic.

The character of pore fluids, which could have effectively leached aluminum from the chloritic layers, can be approximated through evaluating mineral stability relations at 25°C and one atmosphere pressure. Because this requires free energy of formation data for the layered silicates, the stability relations are constructed with idealized clay compositions. The chlorite interlayers will be treated as the clinochlore endmember, $Mg_5Al_2Si_5O_{10}(OH)_8$, and smectite interlayers as saponite, $[Mg_{0.165}]_{ex}$-$Mg_3Al_{0.33}Si_{3.67}O_{10}(OH)_2$, with magnesium in exchangeable sites.

Tardy and Garrels (1974) have described an ingenious method for estimating free energies of formation for layered silicates. They derived the free energies for both the "silicated" cation oxides and hydroxides which are integral parts of the clay structure, and the free energies for "exchangeable" cations (treated as oxides) which occur in less tightly bonded interlayer exchange sites. The appropriate free energies of the cation oxides/hydroxides are then summed in proportion to a given clay composition to yield an estimated value for that clay's free energy of formation.

Unfortunately, this approach had to be abandoned for two reasons. First, the composition of the two idealized 1:1 mixed-layer clays, $(Mg_{0.165}]_{ex}Mg_8Al_{2.33}Si_{6.67}O_{20}(OH)_{10}$ for interstratified clinochlore-saponite and $[Mg_{0.165}]_{ex}$-$Mg_6Al_{0.33}Si_{7.67}O_{20}(OH)_4$ for interstratified talc-saponite, yield calculated free energies whose difference is identical to the free energy difference between discrete clinochlore and discrete talc. Tardy and Garrels (1974) did not consider the free energy contribution to a given discrete clay species when it occurs in a mixed-layer phase. Second, and of more concern, their calculated free energy of formation value for clinochlore (−1958.7 kcal/mol) is more positive than their modified value (−1961.8 kcal/mol) from Helgeson (1969) and substantially more positive than Zen's (1972) value (−1974.0 kcal/mol). The discrepancy may reflect the unique structure of chlorite. A well-defined brucite-like sheet rather than a loosely bound collection of exchangeable cations occupies the interlayer position. The free energy of formation values of the constituent oxides or hydroxides in a chlorite's brucite-like sheet are likely to differ appreciably from either their "silicated" or "exchangeable" equivalents.

Thus, free energy values for the clays in this transformation must be confined to pure endmember clay species,

that is, the free energy of reaction for the discrete clinochlore equilibrium with discrete talc. Several free energy values for talc have been reported (Bricker et al. 1973; Hostetler et al. 1971; Mel'nik, 1972; Parker et al. 1971; Robie et al. 1978) that range from −1324.8 to −1319.0 kcal/mol. The mean value of these (−1322.0 kcal/mol) is arbitrarily selected for this discussion. Only two values for chlorite (clinochlore) were located: Helgeson's (1969) value, subsequently corrected to −1961.8 kcal/mol (Tardy and Garrels, 1974), and Zen's (1972) value of −1974.0 kcal/mol. The large difference between the two values is disturbing, but the mean value of −1967.9 kcal/mol is reluctantly adopted.

These values for the layered silicates and values from Robie et al. (1978) and Hemingway et al. (1978) for other species in the reaction

$$\tfrac{1}{2}Mg_5Al_2Si_3O_{10}(OH)_8 + \tfrac{1}{2}H_4SiO_{4\,aq} + 5H^+_{aq} = \tfrac{1}{2}Mg_3Si_4O_{10}(OH)_2 + Mg^{2+}_{aq} + Al^{3+}_{aq} + 5H_2O \quad (1)$$

yield

$$\log K = 21.9 = \log a^{3+}_{Al} + \log a^{2+}_{Mg} + 5\,pH + 5\log a_{H_2O} - 0.5\log a_{H_4SiO_4} \quad (2)$$

at 25°C and one bar pressure.

To evaluate aluminum activity relations, two additional constraints must be imposed. First, quartz coexists with the layered silicates at equilibrium. This allows calculating dissolved silica activity as a function of water activity through

$$SiO_2 + 2H_2O = H_4SiO_{4\,aq}$$

with

$$\log K = -4.1 = \log a_{H_4SiO_4} - 2\log a_{H_2O} \quad (3)$$

at standard conditions. Second, although redundant for this model, discrete talc also occurs at equilibrium with the clays. This permits calculating the magnesium activity in the fluid in terms of pH and water activity through

$$\tfrac{1}{3}Mg_3Si_4O_{10}(OH)_2 + 2H^+_{aq} = \tfrac{4}{3}SiO_2 + Mg^{2+}_{aq} + \tfrac{4}{3}H_2O$$

with

$$\log K = 12.1 = \log a^{2+}_{Mg} - \tfrac{4}{3}\log a_{H_2O} + 2\,pH \quad (4)$$

at standard conditions. Both constraints are reasonably compatible with the observed mineralogy; commonly quartz and occasionally discrete talc occur in both the chloritic and talc-bearing mixed-layer assemblages.

Equation (2) can now be evaluated in terms of a^{3+}_{Al} vs pH at arbitrarily assigned water activities. The stability relations for reaction (1) are shown on Figure 14 with an equilibrium curve constructed for each of four water activities,

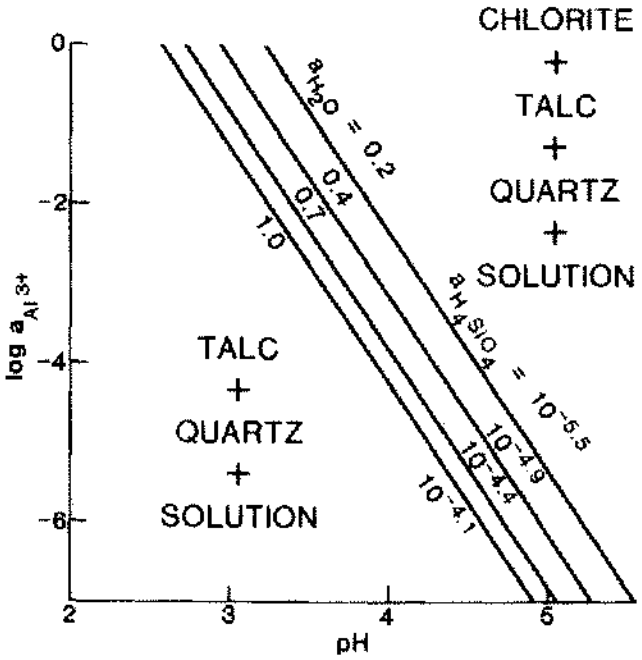

Figure 14. Stability diagram for the talc-chlorite equilibrium at 25°C and 1 bar pressure as a function of a^{3+}_{Al} and pH at water activities of 1.0, 0.7, 0.4, and 0.2; magnesium ion and dissolved silica activities fixed by quartz-talc equilibrium.

1.0, 0.7, 0.4, and 0.2, at 25°C and one atmosphere pressure. The diagram is restricted to the low pH range appropriate for marine bitterns where Al^{3+} activity increases rapidly with decreasing pH and where Al^{3+} is the dominant aluminum species in solution. It is stressed again that because of the use of arbitrarily assigned free energy values for talc and, in particular, chlorite, and because of the inability to include any contribution of "free energy of mixed layering," the positioning of the equilibrium curves is an approximation. The slopes of the curves and their relative positions are valid and illustrate the character of the equilibrium.

Fluids with aluminum ion activity substantially higher than silica activity are restricted to the lower pH region of Figure 14. In a bittern with a pH of 4.4, for example, the a^{3+}_{Al} is less than one-fourth the $a_{H_4SiO_4}$ at water activity of 0.7 (a marine brine precipitating halite); at a water activity of 0.4 (a marine brine in equilibrium with carnallite-kieserite-kainite-halite), however, the a^{3+}_{Al} is more than three times greater than $a_{H_4SiO_4}$ at the same pH. With pH reduced to 4.0 the enhancement of a^{3+}_{Al} is more striking; with a_{H_2O} at 0.7, a^{3+}_{Al} is three times greater than $a_{H_4SiO_4}$, and with a_{H_2O} reduced to 0.4, it becomes 50 times greater. Although these examples cannot be rigorously applied, they clearly point out that the combined effect of lowering pH and reducing water activity can yield a fluid in which the alumina in chlorite is substantially more soluble than silica. Such a fluid, if undersaturated with alumina, or

both alumina and silica, will selectively leach aluminum from chlorite and leave a talc residue.

No attempt is made here to suggest the mechanism of the leaching process. It could range from a strictly solid state transformation by solid diffusion, through dissolution of the chlorite's brucite-like interlayer sheet followed by diffusion in and out of the remnant silicate framework, to complete dissolution of the chlorite and precipitation of talc. The latter process does appear somewhat unlikely because retention of the smectite mixed layering becomes difficult.

Regardless of the mechanism of the replacement process, the occurrence of brines capable of selectively leaching aluminum from the chloritic layers of the interstratified clay is not unreasonable. The speculation that the chlorite layers were leached of aluminum to form talc layers during an episode of brine migration and extensive sulfate recrystallization appears plausible.

REFERENCES

Adams, S. S. 1969. Bromine in the Salado Formation, Carlsbad potash district. New Mexico Bur. Mines and Mineral Resources Bull. 93, 122 p.

Alling, H. L. and L. I. Briggs, Jr. 1961. Stratigraphy of Upper Silurian Cayugan evaporites. Amer. Assoc. Petroleum Geologists Bull. v. 45:515–547.

Anderson, R. Y. 1982. Deformation dissolution potential of bedded salt, Waste Isolation Pilot Plantsite, Delaware Basin, New Mexico: In: Scientific Basis for Radioactive Waste Management-V: New York, Elsevier Scientific Publishing, p. 449–458.

Anderson, R. Y., W. E. Dean, D. N. Kirkland and H. I. Snider. 1972. Permian Castile varved evaporite sequence West Texas and New Mexico. Geol. Soc. America Bull. v. 83:59–86.

Bailey, S. W. 1982. Nomenclature for regular interstratifications. Am. Mineralogist v. 67:394–398.

Bodine, M. W., Jr. 1971. Recent sediments in a hypersaline brine lake, St. Maarten, Lesser Antilles (abs.). EOS (Am. Geophys. Union Trans.), v. 52:854.

Bodine, M. W., Jr. 1976. Magnesium hydroxychloride: A possible pH buffer in marine evaporite brines. Geology v. 4:76–80.

Bodine, M. W., Jr. 1978. Clay-mineral assemblages from drill core of Ochoan evaporites, Eddy County, New Mexico: New Mexico Bur. Mines and Mineral Resources Circ. 159:21–31.

Bodine, M. W., Jr. and B. F. Rueger. In press. Progress report on clay-mineral assemblages in the Gibson Dome No. 1 drill core, Paradox Basin, Utah: U.S. Geol. Survey Open-File Rept.

Bodine, M. W., Jr. and R. R. Standaert. 1977. Chlorite and illite compositions from Upper Silurian rock salts, Retsof, New York. Clays and Clay Minerals, v. 25:57–71.

Borchert, Hermann and R. O. Muir. 1964. Salt Deposits: London, D. Van Norstrand, 338 p.

Braitsch, Otto 1971. Salt Deposits, their Origin and Composition: New York, Springer-Verlag, 297 p.

Bricker, O. P., H. W. Nesbitt and W. D. Gunter. 1973. The stability of talc. Am. Mineralogist v. 58:64–72.

Brindley, G. W. and George Brown, editors. 1980. Crystal Structure of Clay Minerals and their X-ray Identification: London. Mineralog. Soc. Mon. 5, 495 p.

Carroll, Dorothy 1970. Clay Minerals: a Guide to their Identification. Geol. Soc. America Spec. Paper 126, 80 p.

Dellwig, L. F. and R. Evans. 1969. Depositional processes in Salina salt of Michigan, Ohio, and New York. Am. Assoc. Petroleum Geologists Bull. v. 53:949–956.

Dreizler, Ingo 1962. Mineralogische Untersuchungen an zwei Gipsvorkommen der Werraserie (Zechstein). Beitr. Mineralogie u. Petrographie v. 8:323–338.

Droste, J. B. 1963. Clay mineral composition of evaporite sequences *in* Symposium on Salt, Northern Ohio Geol. Soc., p. 56–63.

Eberl, D. D., B. F. Jones and H. N. Khoury. 1982. Mixed-layer kerolite/stevensite from the Amargosa Desert, Nevada. Clays and Clay Minerals, v. 30:321–326.

Echle, Wolfram 1961. Mineralogische Untersuchungen an Sedimenten des Steinmergelkeupers und der Roten Wand aus der Umgebung von Göttingen. Beitr. Mineralogie u. Petrographie v. 8:28–59.

Foster, M. D. 1962. Interpretation of the composition and a classification of the chlorites: U.S. Geol. Survey Prof. Paper 414-A, p. 1–33.

Friedman, G. M. 1965. Occurrence of talc as a clay mineral in sedimentary rocks. Nature v. 207:283–284.

Füchtbauer, H. and H. Goldschmidt. 1959. Die Tonminerale der Zechsteinformation. Beitr. Mineralogie u. Petrographie v. 6:320–345.

Grim, R. E. 1968. Clay Mineralogy (2nd ed.): New York, McGraw-Hill Book Co., 596 p.

Helgeson, H. C. 1969. Thermodynamics of hydrothermal systems at elevated temperatures and pressures. Am. Jour. Sci. v. 267:729–804.

Helgeson, H. C. and F. T. Mackenzie. 1970. Silicate-seawater equilibria in the ocean system. Deep-Sea Research, v. 17:877–894.

Hemingway, B. S., R. A. Robie and J. A. Kittrick. 1978. Revised values for Gibbs free energy of formation of [Al(OH)4-aq], diaspore, boehmite, and bayerite at 298.15 K and 1 bar pressure, the thermodynamic properties of kaolinite to 800 K and 1 bar, and the heats of solution of several gibbsite samples. Geochim. et Cosmochim. Acta, v. 42:1533–1543.

Hemley, J. J., J. W. Montoya, C. L. Christ and P. B. Hostetler. 1977. Mineral equilibria in the MgO-SiO_2-H_2O system: I Talc-chrysotile-fosterite-brucite stability relations. Am. Jour. Sci. v. 277:322–351.

Herrmann, A. G., Doris Knake, Jürgen Schneider and Heide Peters. 1973. Geochemistry of modern seawater and brines from salt pans: Main components and bromine distribution. Contr. Mineralogy and Petrology v. 40:1–24.

Hite, R. J. 1960. Stratigraphy of the saline facies of the Paradox Member of the Hermosa Formation of southeastern Utah and

south-western Colorado, *in* Geology of the Paradox Basin Fold and Fault Belt, 3rd Field Conference: Durango, Colorado, Four Corners. Geol. Soc., p. 86–89.

Hite, R. J. and D. H. Buckner. 1981. Stratigraphic correlations, facies concepts, and cyclicity in Pennsylvanian rocks of the Paradox Basin, *in* Rocky Mountain Assoc. of Geologists, 1981 Field Conference, Guidebook to the Paradox Basin, p. 147–159.

Hostetler, P. B., J. J. Hemley, C. L. Christ and J. W. Montoya. 1971. Talc-chrysotile equilibrium in aqueous solutions. Geol. Soc. America Abstracts with Programs, v. 3:605.

Hower, John, E. V. Eslinger, M. E. Hower and E. A. Perry. 1976. Mechanism of burial metamorphism of argillaceous sediment: Mineralogical and chemical evidence. Geol. Soc. America Bull. v. 87:725–737.

Jones, B. F. and A. H. Weir. In press. Clay minerals in an alkaline saline lake. Clay and Clay Minerals.

Jones, C. L. 1973. Salt deposits of the Los Medanos area, Eddy and Lea Counties, New Mexico: U.S. Geol. Survey Open-file Report USGS-4339-7, p. 1–40.

Khoury, H. N., D. D. Eberl and B. F. Jones. 1982. Origin of magnesium clays from the Amargosa desert, Nevada. Clays and Clay Minerals, v. 30:327–336.

Kühn, Robert 1968. Geochemistry of the German potash deposits: Geol. Soc. America Spec. Paper 88, p. 427–504.

Lambert, S. J. 1978. Geochemistry of Delaware basin ground waters: New Mexico Bur. Mines and Mineral Resources Circ. 159:33–38.

Lippmann, F. and M. Y. Savascin. 1969. Mineralogische Untersuchungen an Lösungsrückständen eines württenbergischen Keupergipsvorkommens. Tschermaks Mineralog. u. Petrog. Mitt. v. 13:165–190.

Lounsbury, R. W. 1963. Clay mineralogy of the Salina Formation, Detroit, Michigan. In: Symposium on Salt, Northern Ohio Geol. Soc., p. 56–63.

Mel'nik, Y. P. 1972. Thermodynamic Constants for the Analysis of Conditions of Formation of Iron Ores: Kiev, Ukranian S. S. R., Institute of Chemistry and Physics of Minerals, Academy of Sciences, 193 p. (in Russian).

Millot, Georges 1970. Geology of Clays: New York, Springer-Verlag, 429 p.

Niemann, Hans 1960. Untersuchungen am Grauen Salzton der Grube "Königshall-Hinderburg", Reyerhausen bei Göttingen. Beitr. Mineralogie u. Petrographie v. 7:137–165.

Parker, V. B., D. D. Wagman and W. H. Evans. 1971. Selected Values of Chemical Thermodynamic Properties, Tables for Alkaline Earth Elements (Elements 92 through 97 in the Standard Order of Arrangement): Natl. Bur. Standards (U.S.), Tech. Note 270–6, 119 p.

Perry, E. A., Jr. 1971. Silicate-seawater equilibria in the ocean system: a discussion. Deep-Sea Research, v. 18:921–924.

Peterson, N. M. A. 1961. Expandable chloritic clay minerals from Upper Mississippian carbonate rocks of the Cumberland Plateau in Tennessee. Am. Mineralogist v. 46:1245–1269.

Pettijohn, F. J. 1975. Sedimentary Rocks (3rd ed.): New York, Harper & Row, 628 p.

Powers, D. W., S. J. Lambert, S. E. Shaffer, L. R. Hill and W. D. Weart, eds. 1978. Geological Characterization Report, Waste Isolation Pilot Plant (WIPP) Site, Southeastern New Mexico: Albuquerque, New Mexico, Sandia Laboratories, SAND 78-1596, 2 vols.

Pundeer, G. S. 1969. Mineralogy, genesis and diagenesis of a brecciated shaley clay from the Zechstein evaporite series of Germany. Contr. Mineralogy and Petrology v. 23:65–85.

Raup, O. B., R. J. Hite and H. L. Groves. 1970. Bromine distribution and Third Symposium on Salt. Northern Ohio Geol. Soc., p. 40–47.

Register, J. B. 1981. Rhubidium-strontium and related studies of the Salado Formation, southeastern New Mexico: Sandia National Laboratories, SAND81-7072, UC-70, 119 p.

Reynolds, R. C. 1980. Interstratified clay minerals, *in* Brindley, G. W. and George Brown, eds. Crystal Structures of Clay Minerals and their X-ray Identification: London, Mineralog. Soc. Mon. 5:249–304.

Rickard, L. V. 1969. Stratigraphy of the Upper Silurian Salina Group, New York, Pennsylvania, Ohio, Ontario: New York State Mus. and Sci. Service, Map and Chart Ser. 12.

Robie, R. A., B. S. Hemingway and J. R. Fisher. 1978. Thermodynamic properties of minerals and related substances at 298.15 K and 1 bar (105 Pascals) pressure and at higher temperatures: U.S. Geol. Survey Bull. 1452, 456 p.

Stewart, F. H. 1963. Marine evaporites: U.S. Geol. Survey Prof. Paper 440-Y, 52 p.

Tardy, Yves and R. M. Garrels. 1974. A method of estimating the Gibbs energies of formation of layer silicates. Geochim. et Cosmochim. Acta v. 38:1101–1116.

Weaver, C. E. and L. N. Pollard. 1973. The Chemistry of Clay Minerals: New York, Elsevier Scientific Publishing, 213 p.

Woodward-Clyde Consultants 1982. Geologic Characterization Report for the Paradox Basin Study Region, Utah Study Areas, Vol. II, Gibson Dome: Office of Nuclear Waste Isolation, ONWI-290.

Zen, E-An. 1972. Gibbs free energy, enthalpy, and entropy of ten rock-forming minerals: Calculations, discrepancies, implications. Am. Mineralogist v. 57:524–553.